Intrinsic ferromagnetism in hexagonal boron nitride nanosheets

M. S. Si, Daqiang Gao, Dezheng Yang, Yong Peng, Z. Y. Zhang, Desheng Xue, Yushen Liu, Xiaohui Deng, and G. P. Zhang

Citation: The Journal of Chemical Physics **140**, 204701 (2014); doi: 10.1063/1.4879055
View online: http://dx.doi.org/10.1063/1.4879055
View Table of Contents: http://scitation.aip.org/content/aip/journal/jcp/140/20?ver=pdfcov
Published by the AIP Publishing

Intrinsic ferromagnetism in hexagonal boron nitride nanosheets

M. S. Si,[1] Daqiang Gao,[1,a)] Dezheng Yang,[1] Yong Peng,[1] Z. Y. Zhang,[1] Desheng Xue,[1,a)] Yushen Liu,[2] Xiaohui Deng,[3] and G. P. Zhang[4]

[1]*Key Laboratory for Magnetism and Magnetic Materials of the Ministry of Education, Lanzhou University, Lanzhou 730000, China*

[2]*Jiangsu Laboratory of Advanced Functional Materials and College of Physics and Engineering, Changshu Institute of Technology, Changshu 215500, China*

[3]*Department of Physics and Electronic Information Science, Hengyang Normal University, Hengyang 421008, China*

[4]*Department of Physics, Indiana State University, Terre Haute, Indiana 47809, USA*

(Received 6 March 2014; accepted 7 May 2014; published online 22 May 2014)

Understanding the mechanism of ferromagnetism in hexagonal boron nitride nanosheets, which possess only *s* and *p* electrons in comparison with normal ferromagnets based on localized *d* or *f* electrons, is a current challenge. In this work, we report an experimental finding that the ferromagnetic coupling is an intrinsic property of hexagonal boron nitride nanosheets, which has never been reported before. Moreover, we further confirm it from *ab initio* calculations. We show that the measured ferromagnetism should be attributed to the localized π states at edges, where the electron-electron interaction plays the role in this ferromagnetic ordering. More importantly, we demonstrate such edge-induced ferromagnetism causes a high Curie temperature well above room temperature. Our systematical work, including experimental measurements and theoretical confirmation, proves that such unusual room temperature ferromagnetism in hexagonal boron nitride nanosheets is edge-dependent, similar to widely reported graphene-based materials. It is believed that this work will open new perspectives for hexagonal boron nitride spintronic devices. © *2014 AIP Publishing LLC*. [http://dx.doi.org/10.1063/1.4879055]

I. INTRODUCTION

It has been theoretically suggested that pure 2D lattices could not survive at any finite temperature owing to thermal fluctuations.[1] The successful preparation of graphene is thus a breakthrough and directly challenges this theory, resulting in a subsequent research focus in condensed matter physics.[2,3] At the same time, this finding attracts fundamental scientific interest,[4] as it holds promising for applications in spintronics where the propagation direction of electrons is robustly linked to their spin orientation.[5–7] The possibility of those nanoscale spintronic devices built around the spin-polarized states at edges of *d*-free layered materials requires a long-range magnetic ordering at finite temperature.[8] However, a predicted magnetic ordering length of about 1 nm is not strong enough to manipulate the electron spin in these graphene-related spintronic devices.[9] From this perspective, great efforts have been devoted to search for other alternative materials. Hexagonal boron nitride (h-BN) is likely to be a potential candidate as the intrinsic nitrogen vacancy can induce a surprising long-range magnetic interaction.[10] In particular, h-BN is well suited for integration with graphene as their lattice constants mismatch is less than 2%.[11] Most importantly, h-BN is a wide-gap semiconductor, which is transferred more easily to the semiconducting field.[12]

Although monolayer h-BN has been studied for about two decades,[13] the multilayer forms have advantages for applications. Many growth techniques that are most likely to scale up to device production naturally produce few-layer h-BN.[14–23] As expected, many unusual properties of few-layer h-BN should be well understood. But, this is not the case for the intrinsic magnetism of few-layer h-BN. This is because only *s* or *p* electrons contributing to the magnetic signal in layered h-BN directly challenges the conventional condensed magnetic phases of 3*d* or 4*f* transition metals. At present, a number of factors are thought to possibly give rise to the magnetic state in h-BN systems: defects in the atomic network,[24–29] ferromagnetic substrates induced magnetism,[30–32] and bared edge localized states.[33–35] Among these factors the defect-mediated mechanism appears to be a difficult one because negatively curved regions can hardly be found in layered h-BN, which is not the focus of this paper. At the same time, the ferromagnetic substrate is an alternative approach to induce magnetism in h-BN. But this is not our case in this work. As for the third scenario, although localized magnetism resulting from strong electron-electron interactions[36] can give rise to ferromagnetic and antiferromagnetic couplings respectively at the N- and B-zigzag edges.[33] Unfortunately, direct experimental evidence supporting such unusual magnetism in layered h-BN is still lacking.

In this work, we confirm the ferromagnetism as an intrinsic property of h-BN nonasheets in experiment for the first time. In addition, we further explicitly show that this ferromagnetic coupling stems from the spin-polarized edges by performing *ab initio* calculations. Theoretical simulations illustrate that only N atoms undeformed at the zigzag edges result in a strong ferromagnetic coupling. Atomic distortions

a)Electronic addresses: gaodq@lzu.edu.cn and xueds@lzu.edu.cn

appear at the armchair edges, where the original hexagonal rings are changed into the deformed pentagonal ones. These predicted ferromagnetic ordering and the distorted pentagonal rings at the armchair edges in h-BN nanosheets coincide with our experimental observations. Most importantly, a high Curie temperature well above room temperature is obtained, consistent with the prediction of Heisenberg model Hamiltonian. It is believed that our systematical work on the h-BN nanosheets may open new perspective for next-generation spintronic devices.

In the rest of this paper, we give a brief explanation of methods in Sec. II. In Sec. III, we present the results and discussion. Section IV is devoted to conclusions.

II. METHODS

In experiment, few-layer h-BN nanosheets were exfoliated from its bulk through using a mechanical cleavage approach. The detailed preparation processes are as follows: first, a sonicate method was used to disperse 1 *g* of BN bulk in 100 mL N,N-Dimethylformamide (DMF) for 10 h. After precipitation, the white dispersion was centrifuged at 2000 rpm for about 20 min to remove the residual large-size powders. Second, the remainder solution was centrifuged at 10 000 rpm for 1 h to obtain the products. To remove the excess surfactant, the samples were repeatedly washed with ethanol and centrifuged. Finally, the samples were dried at 60°C in vacuum condition. It is noted that the powders of sample were taken for the magnetization measurements.

Our *ab initio* calculations are based on DFT using the SIESTA code.[37] The generalized gradient approximation Perdew-Burke-Ernzerhof (PBE) exchange-correlation functional[38] and norm-conserving pseudopotentials are used. The planewave energy cutoff is set to be 400 Ry to ensure the convergence of the calculations. The $1\times1\times1$ for the Monkhorst-Pack *k*-point mesh is used in the calculation. The conjugate gradient algorithm is adopted to fully relax the geometry until the force on any individual atom is less than 0.02 eV/Å. The optimized double-ζ orbitals including polarization orbitals are employed to describe the valence electrons. The Gaussian smearing method is taken in the calculation of density of states (DOS). As a check, we optimize the lattice constant for the monolayer infinite h-BN sheet. The obtained value of 2.511 Å, in a good agreement with the previous theoretical value of 2.511 Å.[39] In addition, we calculate the corresponding formation energy as $E_{\text{form}} = E_{\text{tot}} - \mu[B] - \mu[N]$ with E_{tot} being the total energy of monolayer h-BN, $\mu[B]$ the energy of boron atom in the α rhombohedral phase[40] and $\mu[N]$ the energy of nitrogen atom in the molecular form. The obtained formation energy is about −4.10 eV.

III. RESULTS AND DISCUSSION

A careful caution must be taken into account when one studies the intrinsic ferromagnetism in those *d*-free materials.[41] It should explicitly exclude the introduction of any magnetic impurity at the first place. Thus, a typical mechanical cleavage approach[2] combined with the sonication technology[19] is used to synthesize the desired h-BN

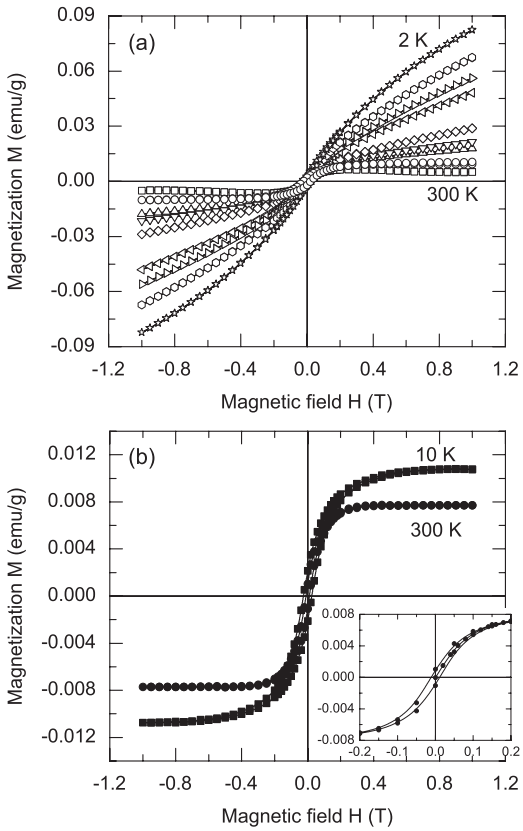

FIG. 1. (a) Magnetization moment M as a function of H for nine temperatures T: 2, 3, 4, 5, 10, 15, 20, 50, and 300 K from top to bottom. (b) Excess magnetization moment M after substracting the paramagnetic and diamagnetic signals as a function of H at $T = 10$ and 300 K, respectively. The inset shows a smaller field region of the hysteresis loop at $T = 300$ K, which behaves a typical ferromagnetic character.

nanosheets (also see the experimental method). The ultrahigh pure h-BN crystals are taken as sources in the preparation process, which leaves little room for ambiguity about the introduction of magnetic impurity.

We begin with the magnetization measurements, which are performed using a SQUID magnetometry. Figure 1(a) plots the *M-H* curves for nine different temperatures T from 2 to 300 K. It clearly shows that h-BN nanosheets exhibit a strong temperature-dependent paramagnetism, originating from the low concentration of individual vacancies introduced near the edges. This paramagnetic feature can be well fitted by the standard Brillouin function and decreases quickly as T increases. In our prepared h-BN nanosheets, such a paramagnetism is negligible above $T = 50$ K. This provides an opportunity to investigate the room ferromagnetism as one can dismiss this involved paramagnetic signal above $T = 50$ K.

It is known that the pristine h-BN crystal is a typical diamagnetic material, which is confirmed in our experiments by measuring its corresponding bulk magnetization curve (not shown for brevity). In our samples, we also observe this temperature-independent diamagnetic signal where the magnetization is inversely proportional to the applied magnetic field. The measured diamagnetic signal stems from the internal perfect hexagonal structure or the bulk's effect. Thus, we can thoroughly eliminate it out of the measured temperature-dependent magnetism. As pointed out above, the paramag-

netism only occurs below $T = 50$ K. Therefore, the room temperature ferromagnetism of h-BN nanosheets can be extracted by only subtracting the diamagnetic contribution at room temperature. In Fig. 1(b), the magnetization loop after subtraction of diamagnetic signal at $T = 300$ K is displayed. It explicitly shows that an indication of ferromagnetic ordering, similar to that reported in graphene-related materials.[42] The obtained saturation magnetization M_S is about 0.008 emu/g at $H = 3000$ Oe, which is quite larger than the value in graphene.[42] The corresponding remanence magnetization is ~0.001 emu/g and the coercivity field is around 114 Oe at room temperature (see the inset in Fig. 1(b)).

As temperature decreases, an enhanced ferromagnetic signal is observed. The saturation magnetization is close to 0.01 emu/g at temperature $T = 10$ K (see the squares in Fig. 1(b)). As a solid check, hysteresis loops were also measured in a wide temperature range 2-400 K. In this temperature range no significant change of the ferromagnetic loops is detected. This implies that the ferromagnetism observed in h-BN nanosheets is generic. Most notably, these h-BN nanosheets should possess a high Curie temperature at least above 400 K, which is of significance for the practical applications of spintronic devices.

To understand the underlying physics of above measured ferromagnetism, let's analyze the sample's lattice. Figure 2(a) shows two representative X-ray diffraction (XRD) curves of the h-BN nanosheets where the XRD of h-BN bulk is given as well for a comparison. The diffraction peaks are well indexed to the hexagonal lattice BN (JCPDS file No. 85-1068). This implies that our prepared samples have the desired hexagonal structure. The (002) peak is the strongest one among these peaks, indicating that the growth of sample is along the *c* axis. However, in the h-BN nanosheets the (002) peak is slightly broadened compared with their bulk, which is due to the presence of slices and distorted edges.[43]

More microscopic structure of h-BN nanosheets is performed by high-resolution transmission electron microscopy (HRTEM) and Cs-corrected TEM, where the water solution of samples are placed on the holey carbon grid in the measurements. Figure 2(b) shows the inner region of h-BN nanosheets at a large scale. The corresponding B-N bond length is determined to be 1.45 Å, in agreement with the known experimental value[44] (see the inset of Fig. 2(b)).

The thinnest region of h-BN nanosheets is close to 1-2 layers from the measurement of atomic force microscopy

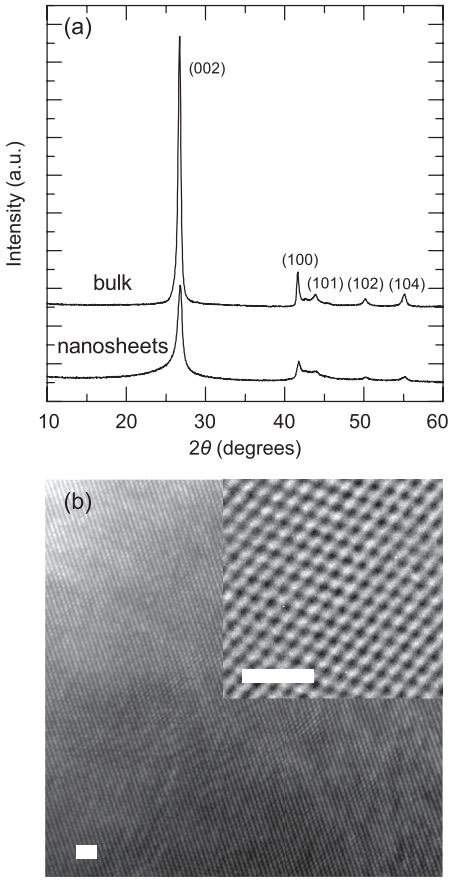

FIG. 2. (a) The power XRD of h-BN bulk and nanosheets. (b) The HRTEM micrograph of h-BN nanosheets at lower magnification. Inset: Large scan Sc-corrected TEM image of internal part, indicating a nice crystallized hexagonal structure. The scale bar is 1 nm.

(AFM) (not shown). But, how h-BN nanosheets exhibit the intrinsic ferromagnetic coupling at room temperature is still not clear from present measurements. It should be noticed that the boundaries exist inevitably in h-BN nanosheets, which will contribute to ferromagnetism, as discussed below.

In order to reveal how magnetism occurs, an *ab initio* simulation is employed, as it is free of any empirical parameter at the atomic scale. However, to mimic the magnetic behavior in practical h-BN nanosheets is not an easy task as at least tens of thousands of atomic orbits are involved. For simplicity, we instead choose a piece of h-BN nanoribbons (h-BNNRs) (see Fig. 3) as our model in the realistic

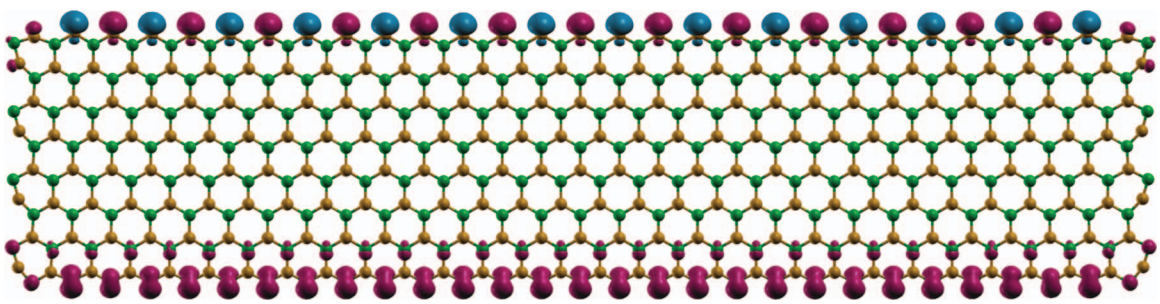

FIG. 3. An optimized piece of h-BN nanoribbon and the corresponding spin density distributions, showing distorted pentagonal rings at the armchair edges and magnetic moment localized mainly at the zigzag edges. Red and blue isosurfaces denote the spin up and spin down, respectively. The isovalue is set to 0.01 μ_B/Borh^3. The yellow and green balls represent boron and nitrogen atoms, respectively.

simulations, which is performed by a fully *ab initio* method (see also Sec. II). Although the weak van der Waals interaction plays a role in the stacking manner of h-BN, it has a negligible effect on magnetic property. This is because the unsaturated bonds at the edges are not connected to its neighbors, which is due to a large interlayer separation. We also shall show that our *ab initio* calculations as well as the Heisenberg model would seem to make possible the explanation of the ferromagnetic ordering in h-BN nanosheets/nanoribbons.

Based on the *ab initio* calculations, we display the optimized configuration of practical h-BNNRs, as illustrated in Fig. 3. Our finding is very insightful. Practical h-BNNRs surprisingly generates a hexagonal-pentagonal ring transition at the armchair edges, which coincides with the previous reports.[45,46] It is emphasized that this hexagonal-pentagonal ring transition is obtained through optimizing the configuration of h-BN nanosheet directly. A natural question is how does this transition happen? Our *ab initio* calculations reveal that the size effect of h-BN BNNRs plays the role in this transition process. As the ribbon's length is smaller than ∼3 nm, no obvious disordered pentagonal rings appear in our simulations. This explains why such a distortion is not predicted in other periodic or small systems.[33] Note that the h-BNNRs in Fig. 3 has the length of 7.2 nm and the width 1.58 nm, which is large enough to mimic our samples in experiments at the first-principles level. On the other hand, the pristine configuration remains unchanged at the neat zigzag edges.

Next, we will show that our above simulation is the direct manifestation of the experimental observation. Thus, a closer inspection of the boundaries is carried out by the Cs-corrected TEM. Our observations match the theoretical predictions. The peculiar disorders did appear at the armchair edges, where the original hexagonal rings were changed into the disordered pentagonal ones, as shown in Fig. 4(a). As the previous work reported in Ref. 14, the normal pentagon formation was excluded in BN systems because the direct B-B and N-N bonds are disfavored. However, in this work we report an alternative formation of pentagonal rings, which originates from the atomic distortions at the armchair edges. Conversely, the zigzag edge behaves a neat feature and the structural configuration remains unchanged (see Fig. 4(b)). All these experimental observations agree well with the *ab initio* simulations, indicating our model used in this work is reliable.

The spin-polarized density is calculated via $\rho_{spin} = \rho_{\uparrow} - \rho_{\downarrow}$ with ↑ and ↓ being the spin up and down, respectively. It clearly shows that the magnetic moments are mainly localized at the zigzag edges, which is in a good agreement with the previous work.[33] The magnetic moments of corresponding B and N atoms are 0.90 and $0.83\mu_B$, respectively. Their respective PDOS are displayed in Fig. 5. It can be seen that the spin polarized states for the B zigzag edge (Fig. 5(a)) appear just below the Fermi energy level. The *s* and *p* orbitals contribute a strong hybridization. This differs from that of N zigzag edges, as shown in Fig. 5(b). Two localized states are spin-splitting near the Fermi level. One is just above the E_F and the other is below the E_F. In addition, the hybridization of *s* and *p* orbitals in these two localized states is very weak. Although those magnetic moments are due to the presence of edge-localized π states close to the Fermi level, the detailed distributions of magnetic moments are also element-dependent: the magnetic moment localized on B atom seems to be a bulb, while that on N atom forms a general dumbbell shape. The bulb-like spin configuration implies that a stronger polarization exists among these edge B atoms, which makes the spin configuration far from the general *p*-orbital configuration. Intriguingly, the distorted armchair edges behave in relatively weak spin-polarized way (see Fig. 3). The B and N atoms in the four corners are also spin-polarized, which generates a maximum magnetic moment of about $0.2\mu_B$. These unusual magnetic moments at the armchair edges are due to the charge redistribution, where the distorted edges play an important role.

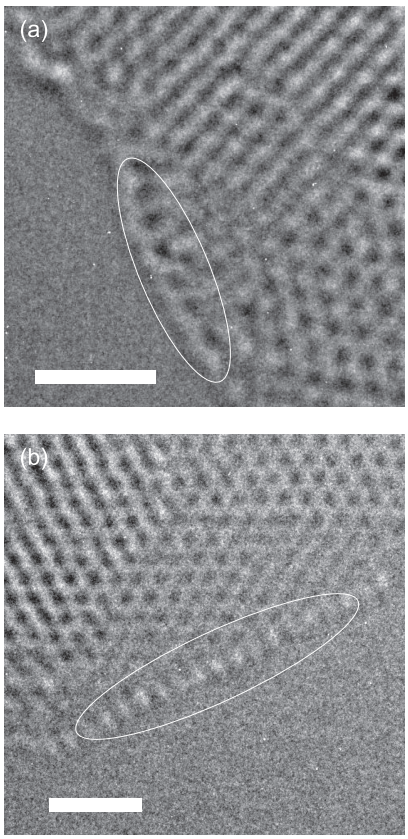

FIG. 4. (a) The distorted pentagonal rings and (b) the nice zigzag edges are detectable. The white ellipses at edges are guide for the eye. The scale bars are set to 1 nm.

To quantify the magnetic interactions, we assume that the energy differences between various magnetic configurations at edges are predominantly caused by the interactions between the B or N moments with spin $\vec{S}$, which can be efficiently modeled by a Heisenberg model with the nearest-neighbor coupling J as, $H = J\sum_{\langle ij\rangle}\vec{S}_i \cdot \vec{S}_j$, where $\langle ij\rangle$ denotes the summation over the nearest neighbors at the zigzag edges and $\vec{S}$ is the net spin of the edge states. Since h-BNNRs are metals derived from semiconductors, this model may miss certain contributions from the itinerant electrons. However, we believe that it grasps the underlying physics on the magnetic orderings. From the calculated energies based on five different spin configurations at the zigzag edges (see Table I), we find that for edge B atoms $J = 11.6$ meV, while

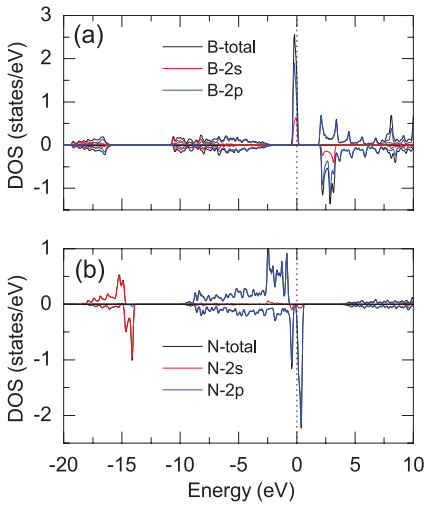

FIG. 5. Projected density of states (PDOS) for (a) B and (b) N atoms at the zigzag edges. The Fermi energy level is set to 0 eV.

for edge N atoms $J = -86.3$ meV. It is known that positive J means an antiferromagnetic coupling, while negative J is ferromagnetic. The magnetic couplings of edge states are indeed element-dependent. The detailed coupling mechanism is totally dominated by the Ruderman-Kittel-Kasuya-Yosida (RKKY) interaction.[49,50] The exchange interaction between the N edge atoms renders a ferromagnetic order, while an antiferromagnetic coupling is formed for the B edge atoms.

Since the antiferromagnetic coupling contributes no net magnetic moment, the ferromagnetic coupling at the N edge dominates the ground state of h-BNNRs (see also Fig. 3). This is the physical origin of room temperature ferromagnetism observed in our experiments. Just recently, new experiment reports the N-terminated zigzag edges in h-BN nanosheets is favorable energetically.[16] This is the direct support of ferromagnetic coupling in h-BN nanosheets. The obtained ferromagnetic exchange parameter J is much larger than that predicted in nitride semiconductors,[10] indicating that the nanostructured h-BN is favorable for promoting a long-range ferromagnetic coupling. The Curie temperature can be judged via $k_B T_C \approx \frac{2}{3} J$ with k_B being the Boltzmann constant.[47] The corresponding estimated theoretical Curie temperature T_C is ~660 K. Indeed, the experimental value is at least above 400 K. Magnetic measurement under a higher temperature will improve this value. Future research can test this prediction directly. Recently, experimental indications of the importance of electron-electron interaction at edges have been reported in graphene nanoribbons.[48] Similarly, such electron-electron interaction in h-BNNRs should be crucial, which might provide the strong magnetic ordering as mentioned above. Thus, the h-BN nanosheets/nanoribbons will be the potential candidates for applications in spintronics because of its room temperature ferromagnetism.

TABLE I. Relative energy E (meV) with respect to the ground state for five spin configurations at the zigzag edges. The spin ground state is referred to (↑↑,↑↓), where the spins are parallel at the N zigzag edge and anti-parallel at the B zigzag edge.

Spin	(↑↑,↑↑)	(↑↑,↓↓)	(↑↓,↑↓)	(↑↓,↑↑)	(↑↑,↑↓)
E	161.9	161.8	1009.9	1369.7	0.0

IV. CONCLUSIONS

In conclusion, we have observed the room temperature ferromagnetism in h-BN nanosheets for the first time, and further clarify this finding based on *ab initio* calculations. It is suggested that the electron-electron interaction located at the edges induces the corresponding magnetic ordering. More importantly, the ferromagnetic ordering at the N-zigzag edges in h-BN nanosheets demonstrates an unexpected high Curie temperature well above room temperature. Our work is believed to provide a solid theoretical foundation for creating new routes in spintronics.

ACKNOWLEDGMENTS

This work was supported by the National Basic Research Program of China under Grant No. 2012CB933101 and the National Science Foundation of China (NSFC) under Grant Nos. 51202101 and 51372107. M.S.S. thanks the State Scholarship Fund by the China Scholarship Council for financially supporting his visit to Indiana State University.

[1]R. E. Peierls, Ann. Inst. Henri Poincare **5**, 177–222 (1935).
[2]K. S. Novoselov, A. K. Geim, S. V. Morozov, D. Jiang, Y. Zhang, S. V. Dubonos, I. V. Grigorieva, and A. A. Firsov, Science **306**, 666–669 (2004).
[3]N. Tombros, C. Jozsa, M. Popinciuc, H. T. Jonkman, and B. J. van Wees, Nature (London) **448**, 571–574 (2007).
[4]C. L. Kane and E. J. Mele, Phys. Rev. Lett. **95**, 146802 (2005); **95**, 226801 (2005).
[5]C. Wu, B. A. Bernevig, and S.-C. Zhang, Phys. Rev. Lett. **96**, 106401 (2006).
[6]D. Pesin and A. H. MacDonald, Nat. Mater. **11**, 409–416 (2012).
[7]A. K. Geim and I. V. Grigorieva, Nat. Mater. **499**, 419–425 (2013).
[8]Y.-W. Son, M. L. Cohen, and S. G. Louie, Nature (London) **444**, 347–349 (2006).
[9]O. V. Yazyev and M. I. Katsnelson, Phys. Rev. Lett. **100**, 047209 (2008).
[10]P. Dev, Y. Xue, and P. Zhang, Phys. Rev. Lett. **100**, 117204 (2008).
[11]B. Sachs, T. O. Wehling, M. I. Katsnelson, and A. I. Lichtenstein, Phys. Rev. B **84**, 195414 (2011).
[12]K. Watanabe, T. Taniguchi, and H. Kanda, Nat. Mater. **3**, 404–409 (2004).
[13]A. Nagashima, N. Tejima, Y. Gamou, T. Kawai, and C. Oshima, Phys. Rev. Lett. **75**, 3918–3921 (1995).
[14]M. Corso, W. Auwärter, M. Muntwiler, A. Tamai, T. Greber, and J. Osterwalder, Science **303**, 217–220 (2004).
[15]W. Auwärter, H. U. Suter, H. Sachdev, and T. Greber, Chem. Mater. **16**, 343–345 (2004).
[16]C. Jin, F. Lin, K. Suenaga, and S. Iijima, Phys. Rev. Lett. **102**, 195505 (2009).
[17]D. Pacilé, J. C. Meyer, C. O. Girit, and A. Zettl, Appl. Phys. Lett. **92**, 133107 (2008).
[18]W. Q. Han, L. Wu, Y. Zhu, K. Watanabe, and T. Taniguchi, Appl. Phys. Lett. **93**, 223103 (2008).
[19]C. Zhi, Y. Bando, C. Tang, H. Kuwahara, and D. Golberg, Adv. Mater. **21**, 2889–2893 (2009).
[20]A. Nag, K. Raidongia, K. P. S. S. Hembram, R. Datta, U. V. Waghmare, and C. N. R. Rao, ACS Nano **4**, 1539–1544 (2010).
[21]L. Song, L. Ci, H. Lu, P. B. Sorokin, C. Jin, J. Ni, A. G. Kvashnin, D. G. Kvashnin, J. Lou, B. I. Yakobson, and P. M. Ajayan, Nano Lett. **10**, 3209–3215 (2010).
[22]J. N. Coleman, M. Lotya, A. O'Neill, S. D. Bergin, P. J. King, U. Khan, K. Young, A. Gaucher, S. De, R. J. Smith, I. V. Shvets, S. K. Arora, G. Stanto,

H.-Y. Kim, K. Lee, G. T. Kim, G. S. Duesberg, T. Hallam, J. J. Boland, J. J. Wang, J. F. Donegan, J. C. Grunlan, G. Moriaty, A. Shmeliov, R. J. Nicholls, J. M. Perkins, E. M. Grieveson, K. Theuwissen, D. W. McComb, P. D. Nellist, and V. Nicolosi, Science **331**, 568–571 (2011).
[23]P. Sutter, J. Lahiri, P. Zahl, B. Wang, and E. Sutter, Nano Lett. **13**, 276–281 (2013).
[24]M. S. Si and D. S. Xue, Phys. Rev. B **75**, 193409 (2007).
[25]M. S. Si, J. Y. Li, H. G. Shi, X. N. Niu, and D. S. Xue, Europhys. Lett. **86**, 46002 (2009).
[26]J. Li, D. Gao, X. Niu, M. S. Si, and D. Xue, Nanoscale Res. Lett. **7**, 624 (2012).
[27]R.-F. Liu and C. Cheng, Phys. Rev. B **76**, 014405 (2007).
[28]A. Du, Y. Chen, Z. Zhu, R. Amal, G. Q. Lu, and S. C. Smith, J. Am. Chem. Soc. **131**, 17354–17359 (2009).
[29]E. Machado-Charry, P. Boulanger, L. Genovese, N. Mousseau, and P. Pochet, Appl. Phys. Lett. **101**, 132405 (2012).
[30]N. Joshi and P. Ghosh, Phys. Rev. B **87**, 235440 (2013).
[31]K. Zumbrägel, K. Wulff, C. Eibl, M. Donath, and M. Hengsberger, Phys. Rev. B **78**, 085422 (2008).
[32]M. N. Huda and L. Kleinman, Phys. Rev. B **74**, 075418 (2006).
[33]B. Barone and J. E. Peralta, Nano Lett. **8**, 2210–2214 (2008).
[34]B. Huang, H. Lee, B.-L. Gu, F. Liu, and W. Duan, Nano Res. **5**, 62–72 (2012).
[35]S. Okada and A. Oshiyama, Phys. Rev. Lett. **87**, 146803 (2001).
[36]M. A. Vozmediano, M. P. Lopez-Sancho, T. Stauber, and F. Guinea, Phys. Rev. B **72**, 155121 (2005).
[37]E. Artacho, E. Anglada, O. Diéguez, J. D. Gale, A. García, J. Junquera, R. M. Martin, P. Ordejón, J. M. Pruneda, D. Sanchez-Portal, and J. M. Soler, J. Phys.: Condens. Matter **20**, 064208 (2008).
[38]J. P. Perdew, K. Burke, and M. Ernzerhof, Phys. Rev. Lett. **77**, 3865–3868 (1996).
[39]Z. Huang, C. He, X. Qi, H. Yang, W. Liu, X. Wei, X. Peng, and J. Zhong, J. Phys. D: Appl. Phys. **47**, 075301 (2014).
[40]L. V. McCarty, J. S. Kasper, F. H. Horn, B. F. Decher, and A. E. Newkirk, J. Am. Chem. Soc. **80**, 2592 (1958).
[41]Y. W. Ma, Y. H. Lu, J. B. Yi, Y. P. Feng, T. S. Herng, X. Liu, D. Q. Gao, D. S. Xue, J. M. Xue, J. Y. Ouyang, and J. Ding, Nat. Commun. **3**, 727 (2012).
[42]P. Esquinazi, D. Spemann, R. Höhne, A. Setzer, K.-H. Han, and T. Butz, Phys. Rev. Lett. **91**, 227201 (2003).
[43]J. C. Meyer, A. Chuvilin, G. Algara-Siller, J. Biskupek, and U. Kaiser, Nano Lett. **9**, 2683–2689 (2009).
[44]B. G. Demczyk, J. Cumings, A. Zettl, and R. O. Ritchie, Appl. Phys. Lett. **78**, 2772–2774 (2001).
[45]M. Topsakal, E. Aktürk, and S. Ciraci, Phys. Rev. B **79**, 115442 (2009).
[46]Y. Ding, Y. Wang, and J. Ni, Appl. Phys. Lett. **94**, 233107 (2009).
[47]J. M. MacLaren, T. C. Schulthess, W. H. Butler, R. Sutton, and M. McHenry, J. Appl. Phys. **85**, 4833–4835 (1999).
[48]C. Tao, L. Jiao, O. V. Yazyev, Y.-C. Chen, J. Feng, X. Zhang, R. B. Capaz, J. M. Tour, A. Zettl, S. G. Louie, H. Dai, and M. F. Crommie, Nat. Phys. **7**, 616–620 (2011).
[49]M. A. Ruderman and C. Kittel, Phys. Rev. **96**, 99 (1954).
[50]K. Yosida, Phys. Rev. **106**, 893 (1957).